Charged particle emission reactions induced by 100-MeV/u ^{12}C ions

Kazuhito Yoshida[1]*, Yuji Yamaguchi[1], Ryota Imamura[1], Tatsuki Kakebayashi[1], Mizuki Yamada[1], Yuki Fukuda[1], Tomoe Katayama[1], Toshiya Sanami[2], Yosuke Iwamoto[3], Naruhiro Matsufuji[4], Yusuke Koba[4], Zviadi Tsamalaidze[5], Petr Evtoukhovitch[5], and Yusuke Uozumi[1]

[1]Department of Applied Quantum Physics and Nuclear Engineering, Kyushu University

[2]High Energy Accelerator Research Organization

[3]Japan Atomic Energy Agency

[4]National Institute for Quantum and Radiological Science and Technology

[5] Joint Institute for Nuclear Research, Dubna, Russia

e-mail: yoshida@nucl.kyushu-u.ac.jp

The measurement was performed at the Heavy Ion Medical Accelerator in Chiba (HIMAC), National Institute for Radiological Sciences, Japan. The carbon-ions were accelerated to 100 MeV/u and bombarded the target (C, Al, and Co). Emitted charged particles were detected by counter-telescopes installed at the PH2. Light particles (p, d, t. ^{3}He and α) were detected with two ΔE-E telescopes comprising two silicon-surface-barrier detectors (SSDs), a GSO(Ce) crystal and four PWO crystals. Particles heavier than α were detected with two ΔE-E telescopes consisting of two SSDs and a CsI(Tl) crystal. Thanks to their high energy resolutions, isotope separation was achieved for many of detected particles. This report describes experimental results obtained during 2018-2019 at HIMAC.

I. INTRODUCTION

With respect to a role in radiotherapy, carbon-ions offer excellent advantages [1]. One is the high relative biological effectiveness (RBE) thanks to its high linear energy transfer (LET). Another advantage of carbon-ion therapy is that it provides highly conformal dose distributions due to the Bragg peak, and therefore it is possible to deliver a large and uniform dose to the target while sparing normal tissues. However, there is a certain potential that they induce undesired dose outside the primary beam field. The undesired dose arises from secondary particles produced through beam interactions with the patient's body. These dose distributions provide a low integral dose to surrounding healthy tissues. The low dose exposure of the normal tissue raised concerns about the occurrence of secondary malignancies as the long-term effects.

When a primary carbon ion traverses the patient body, it can undergo nuclear fragmentation. According to the breakup model [2] and the abrasion-ablation model [3,4], highly energetic particles including clusters, which have approximately same velocities as that of the projectile are observed in the extreme forward cone of laboratory angles. Therefore, they are responsible for the dose tail observed after the distal edge of the Bragg Peak [5,6]. In order to understand the dose tail, many experiments were carried out. The energy-angle double differential cross sections (DDXs) of charged particle productions were also measured [7,8] at angles smaller than 20 degrees including zero degrees. In contrast, little attention has been paid on DDXs of the lateral angles. The charged composite particles, which have high LET and large RBE, emitted laterally have been supposed to have low energies [3,4], and to be stopped within the primary beam diameter. Then, the importance of lateral doses was expected to be negligible. In recent years the increasing concern about low dose exposure requires accurate estimation of lateral doses. However, DDXs of lateral emission of charged composite particles were not reported at larger angles than 20 degrees.

The purpose of this work was to measure DDXs of charged particle emissions to lateral directions from interaction between clinical carbon-ion beam and elements constituting human body. The measurement covered charged particles from protons to 12C, and DDXs were determined for most of isotopes. In this report, we describe the experimental equipment and method, and present some preliminary DDX data measured at the beam energy of 100 MeV/u.

II. EXPERIMENTS

Table 1 Targets used in this work.

III.	Al	C	Co
Thickness [mm]	0.1 and 2.0(for calibration)	0.1	0.05

Experiments were carried out at the Heavy Ion Medical Accelerator In Chiba (HIMAC), National Institute for Radiological Sciences, Japan. ^{12}C beam was focused on a target in a spot of about 5-mm diameter. The target was set at the center of a vacuum chamber of 50-cm diameter. The targets used were ^{12}C, ^{27}Al, and ^{59}Co, which are all natural metals. Their thicknesses is listed in table I.

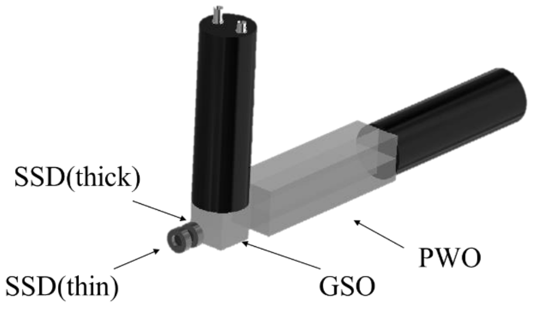

Fig. 1 Telescope for p, d, t, ^{3}He, and α

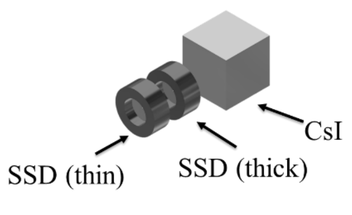

Fig. 2 Telescope for particles heavier than α

The energy of emitted particles was measured with two stacked scintillator spectrometer which are shown schematically in Fig. 1 and Fig.2. Light particles (p, d, t. ^{3}He and α) were detected with two ΔE-E telescopes comprising two silicon-surface-barrier detectors (SSDs), a GSO(Ce) crystal and four PWO crystals. Particles heavier than α were detected with two ΔE-E telescopes consisting of two SSDs and a CsI(Tl) crystal. The first and second SSD were ΔE detectors 100μm and 2mm in thickness, respectively. GSO(Ce) crystal was cubic with an edge length of 43mm. PWO scintillator was cuboidal with 50 × 50 × 199mm. CsI(Tl) scintillator was cubic with an edge length of 28mm.

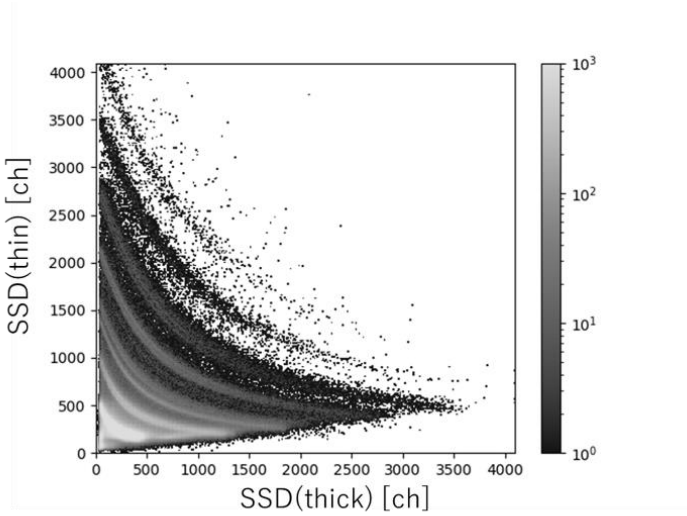

Fig. 3　Two dimensional scatter plot of first and second SSD

The number of incident ^{12}C ions was determined by plastic scintillator placed downstream of the chamber as indirect beam monitor. Then, the plastic scintillator was used to count the number of secondary particles scattered from a thin metal foil to avoid the plastic scintillator pile up. So DDXs of 2.0mm ^{27}Al target was measured with lower beam intensity for calibration and we calibrated incident beam monitor by comparing DDXs of 2.0mm ^{27}Al and 1.0mm ^{27}Al using DDXs.

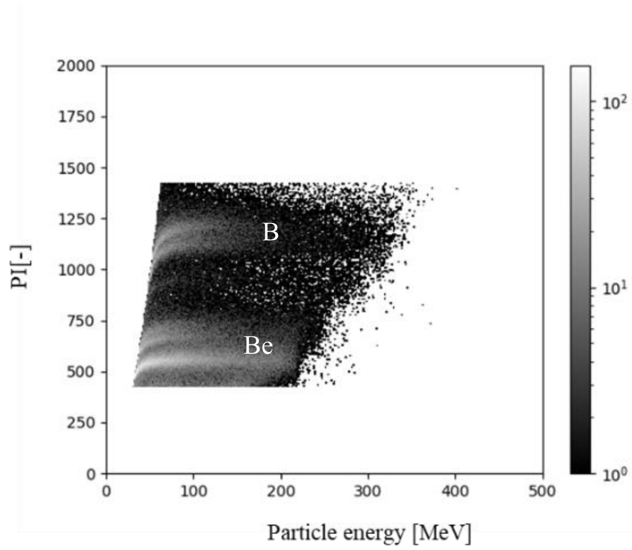

Fig. 4 Two-dimensional plot of PI versus particle energy (Be and B)

Telescope which used for measuring Light particles (p, d, t. ^3He and α) had sufficient depth to stop 480-MeV protons and 1200-MeV α-particles. Fig.3 shows the example data measured by telescope which was consisted of two SSDs and CsI(Tl) scintillator. Telescope which used measuring for particles heavier than α had sufficient depth to stop 730-MeV ^6Li ions and 1200-MeV ^{12}C ions. One of faces of GSO(Ce) scintillator and

PWO scintillator were connected to photomultiplier tube (PMT) and that of CsI(Tl) scintillator was connected to photo diode to convert scintillation light into the electric signal and amplify the signal.

Electric signals from detectors were fed into a spectroscopic amplifier via a preamplifier. Their pulse heights were analyzed by an amplitude-to-digital converter. The digitized data were transferred to a PC through the CAMAC system, and recorded on hard-drive. Energy calibration was performed by referring to proton energy which was calculated by Bethe equations. The spectrometers which was used measuring light particles (p, d, t. ^{3}He and α) was installed outside the chamber. The telescope which was used measuring particles heavier than α was installed into the vacuum chamber. Light particles (p, d, t. ^{3}He and α) energy spectra were measured at laboratory angles from 30◦ to 120◦. Particles heavier than α energy spectra were measured at laboratory angles 15◦ and 20◦.

High-energy particles may undergo nuclear reactions before being stopped or may scatter out of the crystal. The ratio between the number of stopped particles and the total number of particles is referred to as the peak-to-total efficiency of the spectrometer and is necessary to determine absolute cross sections. Thus far, efficiency has been determined as a function simulated by PHITS calculation. The DDXs are determined by

$$\frac{d^2\sigma}{d\Omega d\varepsilon} = \frac{Y}{PS_t\phi\Delta\Omega\Delta\varepsilon},$$

where Δε is the energy bin width required for data reduction, ΔΩ is the solid angle of the detector, P is the peak efficiency, S_t is the surface density of the target, and ϕ is the total charge of the incident ^{12}C beam.

The number of emitted particles in $\Delta\varepsilon$, which is represented by Y, is obtained by the particle identification (PI) technique. The quantity PI is given by

$$\mathrm{PI} = E_{tot}^b - (E_{tot} - \Delta E)^b,$$

where E_{tot} is the total energy deposited in the detector and ΔE is the energy measured in the ΔE detectors. The parameter b is set at 1.73, which is the optimum value to separate isotopes. Two dimensional of PI versus emission energy of Be and B was shown in Fig.6.

IV. RESULT AND DISCUSSION

Preliminary data have been obtained for the reaction of 100-MeV/u ^{12}C ion on the ^{27}Al target. The spectra of DDXs for 100MeV/u ^{27}Al(^{12}C, px) and ^{27}Al(^{12}C, αx) reactions at 30, 45, 60, 120 degrees are shown in Fig.5 and Fig.6, respectively. The spectra of DDXs for 100MeV/u ^{27}Al(^{12}C, ^{7}Bex) reactions at 15, 20 degrees are shown in Fig.7. Maximum energy of proton was 210MeV at 60degrees. The highest observed energy of α-particle was 230MeV at 60 degrees. The highest observed energy of ^{7}Be was 490MeV at 20degrees. α-particle of 230MeV has the range of 28.5-mm in water. Therefore, healthy tissues around the beam axis to cancerous tissues can be affected by such high-energy particles. As shown in Fig.6, 470MeV α-particles were measured at 30degrees. In previous study, 285MeV proton was observed for 400MeV ^{nat}C(α, px) reactions at 30degrees. Considering secondary nuclear reactions, influence of charged particle emission over 30degrees for human cannot ignored.

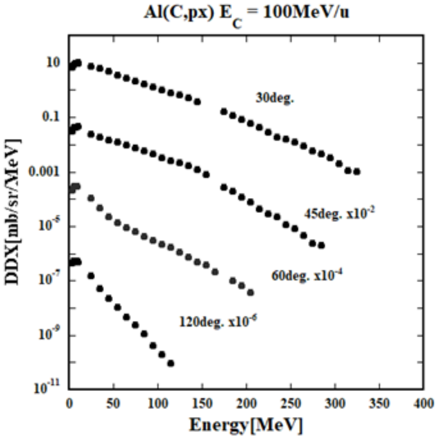

Fig. 5 DDXs of ^{27}Al(^{12}C, px) reaction

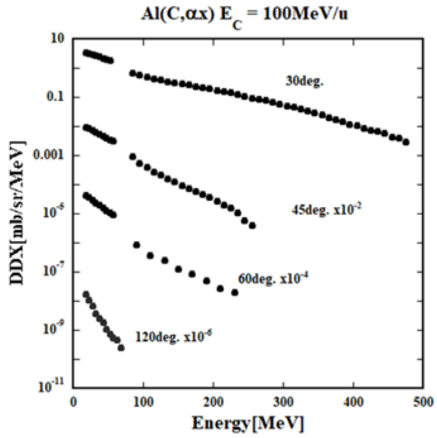

Fig. 6 DDXs of ^{27}Al(^{12}C, αx) reaction

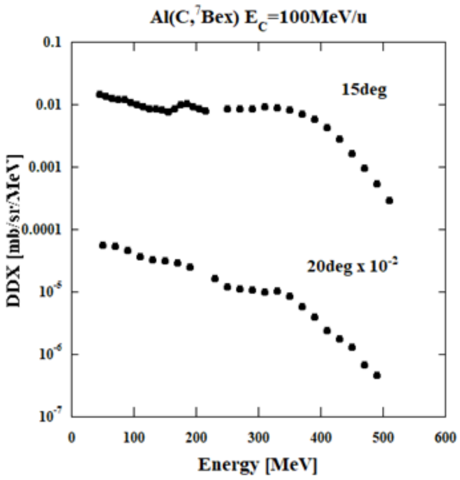

Fig. 7 DDXs of ^{27}Al(^{12}C, ^{7}Bex) reaction

V. CONCLUSION

We measured DDXs of charged particle emission reactions induced by 100MeV/u ^{12}C ions on three targets (C, Al, Co) at 15, 20, 30, 45, 60, and 120 degrees at HIMAC, NIRS. DDXs of emitted particles (p, d, t, ^{3}He, α, ^{6}Li, ^{7}Li, ^{7}Be, ^{9}Be, ^{10}Be, ^{10}B, ^{11}B, ^{10}C, ^{11}C, ^{12}C) were determined in wide ranges of emission energies. The notable point is that high-energy particles are observed at large angles. Particularly,α particles above 100 MeV show certain values of DDXs. This fact suggests that the high-energy heavy-ions can have a long range over the beam diameter, and the healthy tissue around the initial beam axis may have late effects low-dose exposure of heavy ions.

ACKNOWLEDGMENTS

This work was conducted under the research project with heavy ions at NIRS-HIMAC, program number H350. This work was supported by JSPS KAKENHI Grant Number JP17H03522.

REFERENCES

[1] D. Schardt, T. Elsässer, and D. Schulz-Ertner, “Heavy-ion tumor therapy: Physical and radiobiological benefits,” Rev. Mod. Phys. 82, 383 (2010).

[2] J. R. Wu, C. C. Chang, and H. D. Holmgren, “Breakup of α Particles in the Fields of Nuclei,” Phys. Rev. Lett. 40, 1013 (1978).

[3] R. Serber, “Nuclear reactions at high energies,” Phys. Rev: 72; 1114–1115, (1947).

[4] J. Hüfner, K. Schäfer, B. Schürmann, “Abrasion-ablation in reactions between relativistic heavy ions,” Phys. Rev. C12, 1888 (1975).

[5]N. Matsufuji, A. Fukumura and M. Komori et al. “Influence of fragment reaction of relativistic heavy charged particles on heavy-ion radiotherapy,” Phys. Med. Biol., 48, pp. 1605-1623, (2003).

[6] N. Matsufuji, T. Kanai, N. Kanematsu, T. Miyamoto, M. Baba, T. Kamada, H. Kato, S. Yamada, J. Mizoe and H. Tsujii, “Specification of Carbon Ion Dose at the National Institute of Radiological Sciences (NIRS),” J. Radiat. Res: 48; Suppl. A:A81-6 (2007).

[7] M. De Napoli et al., “Carbon fragmentation measurements and validation of the Geant4 nuclear reaction models for hadrontherapy,”, Phys. Med. Biol. 57, 7651-7671 (2012).

[8] M. Toppi et al., “Measurements of ^{12} C ion fragmentation on thin carbon target from the FIRST collaboration at GSI,” Jour. Phys. Conference Series 590, 012035 (2015).